Biochemical and Biophysical Research Communications 398 (2010) 433–437

Contents lists available at ScienceDirect

Biochemical and Biophysical Research Communications

journal homepage: www.elsevier.com/locate/ybbrc

Vinculin's C-terminal region facilitates phospholipid membrane insertion

Volker F. Wirth [a], Felix List [b], Gerold Diez [a], Wolfgang H. Goldmann [a,*]

[a] Center for Medical Physics and Technology, Biophysics Group, Friedrich-Alexander-University, Erlangen-Nuremberg, Erlangen, Germany
[b] Institute of Biophysics and Physical Biochemistry, University of Regensburg, Germany

ARTICLE INFO

Article history:
Received 20 June 2010
Available online 1 July 2010

Keywords:
Vinculin
Vinculin tail: H3 and C-terminus
Lipid-membrane binding
Focal adhesions
Differential scanning calorimetry
Circular dichroism spectroscopy
Tryptophan quenching
Gel electrophoresis

ABSTRACT

The focal adhesion protein vinculin has been implicated in associating with soluble and membranous phospholipids. Here, we investigated the intermolecular interactions of two vinculin tail domains with membrane phospholipids. Previous studies have shown that the tail's unstructured C-terminus affects the mechanical behavior of cells, but not the H3 region. The aim of this work was to establish whether the C-terminal or the H3 region either associate favorably with or anchor in lipid membranes. This work characterizes the energetics and dynamics of phospholipid interactions using differential scanning calorimetry (DSC) as well as circular dichroism (CD) spectroscopy. Biochemical data from tryptophan quenching and SDS–PAGE experiments support calorimetric and CD spectroscopic findings insofar that only vinculin's C-terminus inserts into lipid membranes. These *in vitro* results provide further insight into the mechanical behavior of vinculin tail regions in cells and contribute to the understanding of their structure and function.

1. Introduction

Cell contact to extracellular matrix (ECM) proteins is important for cell adhesion, migration, and survival. Most cell–matrix contacts are linked to the actin filaments *via* the heterodimeric transmembrane protein integrin and the focal adhesion complex (FAC) proteins. Within FAC, a variety of adaptor proteins have been implicated to associate with or in some cases insert into lipid membranes [1]. The focal adhesion protein vinculin shows such lipid binding ability. Two regions on the tail domain have been experimentally identified as candidates for lipid binding: helix 3 (residues 935–978) [2] and the lipid anchor region (residues 1052–1066) [3]. Mutating helix 3 and the unstructured C-terminal arm resulted *in vitro* in impaired lipid vesicle interaction of the vinculin-tail [3]. Pull-down assays with artificial lipid membranes revealed that in contrast to the complete vinculin-tail (Vt), a variant lacking the lipid anchor (vinΔC), does not interact with vesicles [3,4]. In addition, using DSC and CD-spectroscopic measurements showed that the C-terminal anchor has the potential to insert into the hydrophobic core of lipid membranes [5].

More recently, Diez et al. [6] reported that mouse embryonic fibroblasts (MEFs) expressing vinculin without the lipid anchor (residues 1052–1066; vinΔC) showed decreased focal adhesion turnover that resulted in impaired cell adhesion and migration. Further, the influence of the lipid anchor region was determined in mechanical terms in MEFs. Compared to the wildtype, MEFvinΔC cells were less stiff, formed fewer focal contacts and generated less adhesive forces. Attenuated traction forces were also found in cells that expressed vinculin with point mutations in the lipid anchor which had either impaired lipid-membrane binding or were prevented from *src*-kinase phosphorylation at the Y1065 site. However, traction generation was not diminished in MEFs that expressed vinculin with impaired lipid binding on helix 3 as a result of point mutations. These results show that both the lipid binding and the *src*-kinase phosphorylation of vinculin's C-terminus are important for cell mechanical behavior, whilst the lipid binding of helix 3 is not, suggesting that both the lipid anchor and the *src*-kinase phosphorylation of Y1065 may regulate cellular mechanical activities.

In this study, we examined the lipid binding ability of vinculin's tail C-terminal and helix 3 region *in vitro* using differential scanning calorimetry (DSC), tryptophan fluorescence quenching, and SDS–PAGE. Results from these measurements should confirm whether the C-terminal arm and/or helix 3 are directly involved in lipid binding and whether they can insert into the hydrophobic region of lipid membranes. CD-spectroscopy was also applied to investigate the conformational behavior of the C-terminus and H3 region in the presence of lipid membranes.

2. Materials and methods

2.1. Peptide and lipid preparations

All peptides of the vinculin tail domain: (i) helix 3 wildtype (H3wt) = residues 944–972 (KRALIQCAKDIAKASDEVTRLAKEVAKQC);

* Corresponding author. Address: Center for Medical Physics and Technology, Biophysics Group, Friedrich-Alexander-University of Erlangen-Nuremberg, Henkestrasse 91, 91052 Erlangen, Germany. Fax: +49 (0) 9131 85 25601.
E-mail address: wgoldmann@biomed.uni-erlangen.de (W. H. Goldmann).

0006-291X/$ - see front matter © 2010 Elsevier Inc. All rights reserved.
doi:10.1016/j.bbrc.2010.06.094

(ii) helix 3 mutant (H3mut) = residues 944–972 with K952Q, K956Q, R963Q, and K966Q; (iii) C-terminus wildtype (CTwt) = residues 1046–1066 (IKIRTDAGFTLRWVRKTPWYQ); (iv) C-terminus mutant (CTmut) = residues 1046–1066 with R1060Q and K1061Q were synthesized and kindly provided by Dr. Wolfgang H. Ziegler (IZKF, Leipzig) and stored in lyophilized form at −80 °C. The phosphorylated C-terminus (CTph) of pY1065 was purchased from Genaxxon Bioscience, Ulm, Germany. Prior to calorimetric measurements, the peptides were dissolved in a buffer containing 20 mM HEPES, 2 mM EDTA, 5 mM NaCl, and 0.2 mM DTT at pH 7.4. For CD-spectroscopic and fluorescence measurements, the peptides were dissolved in 10 mM potassium phosphate buffer at pH 7.4.

Multilamellar lipid vesicles (MLVs) were prepared from dimyristoyl-L-α-phosphatidylcholine (DMPC) and dimyristoyl-L-α-phosphatidylserine (DMPS) (Avanti Polar Lipids, Birmingham, AL, USA) as described in [5]. In brief, mixtures of DMPC and DMPS or pure DMPC were dissolved in chloroform/methanol at 2:1 (v/v), and the solvent was evaporated by gently agitating the flask under a stream of nitrogen. This was followed by a further 2 h vacuum desiccation. For calorimetric measurements, the lipid film was suspended in the above buffer at a concentration of 10 mg/ml and left overnight at +35 °C (DMPC) and at +45 °C (DMPC/DMPS) for vesicle formation. For CD-spectroscopic experiments, small unilamellar vesicles (SUVs) were used; for that, the lipid film was dissolved in 10 mM potassium phosphate buffer at pH 7.4 and then sonicated until the solution was transparent.

2.2. Differential scanning calorimetry (DSC)

A differential scanning calorimeter Q100 (TA Instruments) was used as described in [5]. In brief, under loosely sealed conditions, lipid solutions in the presence/absence of peptides were heated in a steel cuvette of 100 µl volume at a rate of 0.5 °C/min and cooled at 1 °C/min. The heat capacity was recorded between +7 and +30 °C, using only cycles after the equilibration phase. The phase transition peak, T_m was observed around +23 °C for pure DMPC and DMPC/DMPS. Data analysis was performed using the software *Universal Analysis 2000* (TA Instruments) and *Origin* 7G [7].

2.3. Circular dichroism (CD)-spectroscopy

CD spectroscopy was executed on a JASCO J-815 CD spectrophotometer as described in [5]. In brief, measurements were taken between 190 and 240 nm and recorded at 1 nm interval using a quartz cuvette of 0.1 cm path length. Three spectra of 70 µM peptide solution at a P/L molar ratio of 1:40 were recorded and averaged. These scans were then corrected by subtracting either the traces from the pure buffer or lipid solution (control). To obtain the mean residue molar ellipticity (θ) at each wavelength, the data were then further adjusted for protein concentration and path length. The spectra were also analyzed using the DichroWeb database (http://dichroweb.cryst.bbk.ac.uk).

2.4. Fluorescence quenching

Measurements were done on a CARY ECLIPSE spectrophotometer using a 1 ml quartz cuvette that contained a peptide–lipid composition of 70 µM peptide and at a P/L ratio of 1:40 and +25 °C. Upon addition of 5 × 50 mM acrylamide over 5 min, changes in tryptophan emission were recorded at 355 nm; the excitation wavelength of 295 nm was chosen to reduce the effect of absorption by acrylamide [8]. Quantitative analysis was achieved using the Stern–Volmer relation, $F_o/F = 1 + K_{SV} \times [Q]$ by determining the constant, K_{SV} from the gradient of a linear fit [9].

2.5. Freeze/thaw, centrifugation, and SDS–PAGE

The phospholipid vesicle solutions (DMPC/DMPS, 70:30 at 10 mg/ml) in the presence of 120 µM H3wt, H3mut, CTwt, CTmut, or CTph peptide concentration were subjected to three independent freeze/thaw cycles from +7 to +35 °C. At the end of these cycles, the peptide–liposome solutions were centrifuged at 20,000*g* for 45 min at +4 °C to separate bound from unbound proteins to lipids followed by SDS–PAGE analysis [10]. The reconstitution of these peptides mixed with vesicles was densitometrically determined using the program ImageJ by measuring the intensities, i.e. gray scales of the SDS gel (http://rsb.info.nih.gov/ij/download.html).

3. Results

3.1. Differential scanning calorimetry (DSC)

DSC was used to determine the association/insertion behavior of the vinculin tail peptides H3wt, H3mut, CTwt, CTmut, and CTph at/into artificial phospholipid membranes. Each measurement was performed with MLVs at 5 mg/ml consisting of DMPC/DMPS and at increasing peptide concentration. In Fig. 1A, MLVs at a molar ratio of 70:30 DMPC/DMPS were incubated with the vinculin tail peptides H3wt and H3mut, and the transition enthalpy was determined. With increasing peptide concentration ranging from 0 to 180 µM, the specific heat and phase transition temperature (T_m) of MLVs changed only marginally compared to pure MLVs. The rel-

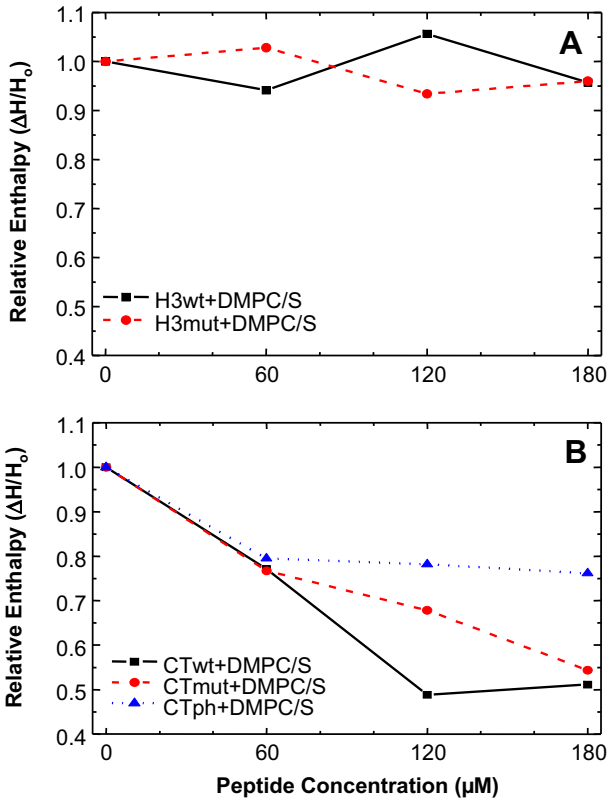

Fig. 1. Vinculin tail peptide interactions with MLVs. DSC measurements were performed with lipid vesicles containing 5 mg/ml DMPC and DMPS at a molar ratio of 70:30. When increasing the peptide concentration from 0 to 180 µM, the relative transition enthalpy ($\Delta H/\Delta H_o$) did not change significantly (±10%) in presence of H3wt and H3mut (A). In contrast, the enthalpy was reduced by lipid insertion of the CT peptides in the following order: CTwt > CTmut > CTph (B). Note, that ΔH_o refers to the transition enthalpy of the lipids at zero peptide concentration and ΔH at the given peptide concentration.

ative transition enthalpy ($\Delta H/\Delta H_o$) of H3wt and H3mut as a function of increasing peptide concentration indicated similar (±10 %) lipid membrane association behavior. In contrast, MLVs in the presence of increasing peptide (CTwt, CTmut, and CTph) concentration showed a relative flattening of the curves together with a shift of T_m to lower temperatures which is indicative for peptide insertion into lipid bilayers [11]. The relative transition enthalpy ($\Delta H/\Delta H_o$) was dramatically reduced with the increase in peptide concentration, whereby the insertion behavior of CTwt and CTmut was more pronounced than for CTph. Note, that the presence of pure DMPC showed no effect at any of the peptides in terms of phase transition (T_m) or transition enthalpy ($\Delta H/\Delta H_o$), indicating that charged liposomes are a requirement for peptide–lipid association/ insertion (data for pure DMPC are not shown).

3.2. Circular dichroism (CD) spectroscopy

The secondary structure of the peptides in the presence/absence of different SUVs was determined using CD-spectroscopic measurements. SUVs consisting of 70% DMPC and 30% DMPS or 100% pure DMPC were used in these experiments. Measuring between 190 and 240 nm, the spectra of the peptides in the presence of pure DMPC lipids showed a minimum at around 200 nm, whilst the presence of DMPC/DMPS had an influence on this minimum. Pure DMPC had little effect on the peptides' secondary structure. Using CTwt peptides in the presence of DMPC/DMPS shifted the spectra to almost 220 nm, whilst the H3wt peptide peaked around 208 nm. These results suggest a change in conformation for CTwt and a smaller change for H3wt peptides. Specifically, the β-sheet conformation remained the same for CTwt in the presence of DMPC/DMPS and showed only an increase in the α-helical conformation, whilst the β-sheet conformation of H3wt was dramatically reduced and the α-helical conformation was significantly increased (Fig. 2A and B). These changes in spectral characteristics for peptides in the presence/absence of lipid vesicles containing DMPC/DMPS support the notion that β-sheet conformations may be responsible for peptide–lipid association/insertion. Table 1 shows the results of the quantitative analyses of all CD spectra (incl. H3mut and CTmut for comparison) using the CDSSTR algorithm provided by Dichroweb [5].

3.3. Fluorescence quenching

The high sensitivity of tryptophan fluorescence in CTwt and CTmut peptides at position 1058 and 1064 allowed fluorescence quenching to be measured directly. Fluorescence quenching was linear with increasing acrylamide concentration. Fig. 3 shows the dependence of tryptophan fluorescence at 355 nm with respect to total acrylamide concentration. The data obtained from steady state titration were analyzed by the Stern–Volmer relation, $F_o/F = 1 + K_{SV} \times [Q]$, where F_o and F are the fluorescence signals for zero and at the given acrylamide concentration, [Q] is the acrylamide concentration, and K_{SV} is the gradient. The fitted line gives a value for K_{SV} of 0.02 for pure CTwt, 0.015 for CTwt in the presence of DMPC, 0.0015 for CTwt in the presence of DMPC/DMPS, 0.017 for pure CTmut, 0.014 for CTmut in the presence of DMPC, and 0.002 for CTmut in the presence of DMPC/DMPS. The data show that the presence of DMPC leads to a slight reduction of the quenching effect (18–25%) for both CTwt and CTmut. However, fluorescence quenching was dramatically impaired in the presence of DMPC/DMPS; it was reduced by 85–93% compared to the quenching level in the absence of lipid vesicles, indicating that the tryptophan residues inserted into the lipid vesicles, and thus were not accessible for the acrylamide molecules. Note, that H3wt and H3mut peptides could not be examined due to the lack of tryptophan residues.

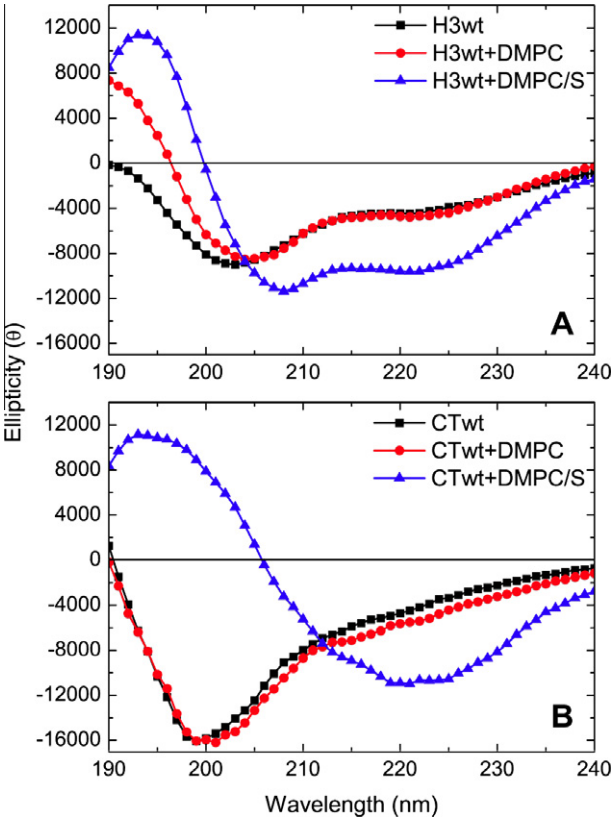

Fig. 2. Results from CD-spectroscopic measurements of H3wt (A) and CTwt (B) peptides in the presence of pure DMPC, DMPC/DMPS (70:30), or in absence of SUVs. The CD spectra at 70 μM peptide were obtained in 10 mM sodium phosphate at pH 7.4 and 25 °C. The values are expressed as mean residue molar ellipticity (θ) in deg cm^2 dmol^{-1}.

Table 1
Results from CDSSTR analyses of H3wt and CTwt in the presence of DMPC, DMPC/DMPS (70:30), or in the absence of lipid vesicles; data for H3mut and CTmut, which are similar to wildtype, are included (shown in italics) for comparison, and significant changes are marked in bold.

System	α-Helix	β-Strand	Turn	Unordered	Total	NRMSD
H3wt	**0.07**	**0.34**	0.14	0.43	0.98	0.023
H3wt + DMPC	0.08	0.36	0.13	0.43	1	0.033
H3wt + DMPC/S	**0.34**	**0.16**	0.14	0.35	0.99	0.018
H3mut	***0.06***	***0.34***	*0.14*	*0.44*	*0.98*	*0.022*
H3mut + DMPC	*0.06*	*0.35*	*0.14*	*0.44*	*0.99*	*0.026*
H3mut + DMPC/S	***0.24***	***0.26***	*0.13*	*0.37*	*1*	*0.021*
CTwt	**0.06**	0.35	0.14	**0.46**	1.01	0.018
CTwt + DMPC	0.08	0.32	0.13	0.46	0.99	0.021
CTwt + DMPC/S	**0.18**	0.34	0.12	**0.36**	1	0.021
CTmut	***0.05***	*0.34*	*0.14*	***0.46***	*0.99*	*0.025*
CTmut + DMPC	*0.04*	*0.24*	*0.15*	*0.52*	*0.95*	*0.067*
CTmut + DMPC/S	***0.22***	*0.32*	*0.11*	***0.34***	*0.99*	*0.023*

3.4. Freeze/thaw, centrifugation, and SDS–PAGE

To further investigate whether vinculin tail peptides were reconstituted into mixed DMPC/DMPS vesicles, unbound and stably incorporated proteins were separated into supernatant (S) and vesicular pellet fractions (P) after centrifugation, respectively. We used 120 μM peptide to test the lipid binding. Fig. 4 supports findings from DSC measurements (cf. Fig. 1B) quantitatively and demonstrates that CTwt, CTmut, and CTph insert into lipid membranes. The results at this concentration show the following pellet/supernatant ratios from two separate experiments for CTwt,

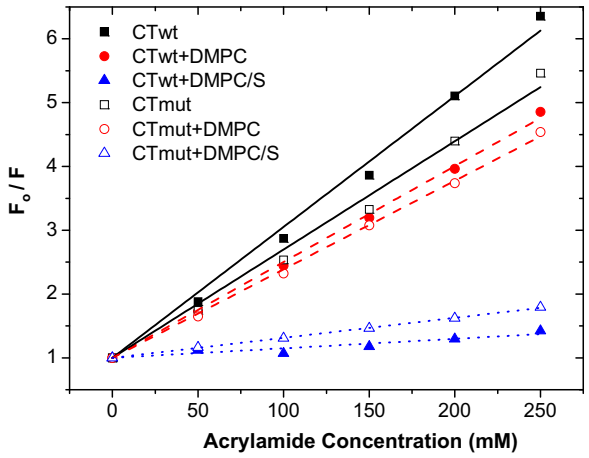

Fig. 3. Tryptophan protein fluorescence quenching. With increasing acrylamide concentration (0–250 mM), the emitted light at 355 nm is quenched according to the relation $F_o / F = 1 + K_{sv} \times [Q]$, where F = protein fluorescence at a given acrylamide concentration, F_o = protein fluorescence at zero acrylamide concentration, K_{sv} = gradient, and $[Q]$ = acrylamide concentration for the peptides CTwt and CTmut in the presence of pure DMPC, DMPC/DMPS (70:30), or in the absence of lipid vesicles.

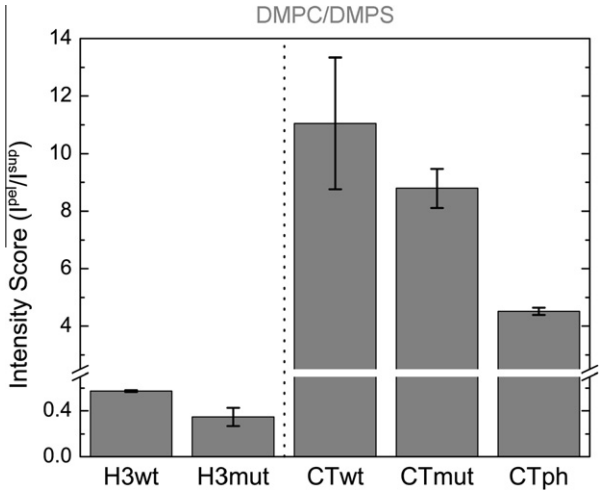

Fig. 4. Intensity score (I^{pel}/I^{sup}) from two densitometric measurements of SDS–PAGE gels of the bound and unbound peptides: H3wt, H3mut, CTwt, CTmut, and CTph in the presence of DMPC/DMPS (70:30).

CTmut, and CTph between 9.4–12.5, 8–9.4, and around 4.5 compared to H3wt and H3mut at around 0.58 and between 0.3 and 0.4, respectively, which indicates that H3wt and H3mut only weakly associate with lipid membranes.

4. Discussion

Force coupling of cell–matrix adhesion is believed to be transduced to the actin cytoskeleton *via* the integrins. The binding of the focal adhesion protein talin to β-integrin's intracellular chain activates the integrin receptor and exposes binding sites for other proteins which includes the recruitment of vinculin to focal adhesion sites [12–15]. Vinculin interacts with both, talin and actin and ensures that there is mechanical stability and a committed regulation of focal adhesions. The control of vinculin levels, specifically the intracellular concentration of recruited functional vinculin, is essential for complexing cytoskeletal and cytoplasmic proteins and is vital for the correct control of cytoskeletal mechanics and the integrity of cell shape [6,16–18].

We and others have previously proposed that vinculin tail binds to lipids and that the tertiary structure of the vinculin tail domain is composed of a typical five helical bundle adopting an anti-parallel topology stabilized by intramolecular hydrogen bonds [4,19,20]. Using site-directed mutagenesis, these researchers illustrated that intermolecular interactions between the vinculin tail and lipids are controlled by two surfaces exposing basic (positively charged) residues called the "collar" and the "ladder" and that the C-terminal (last) residues 1062–1066 (TPWYQ) are directly implicated in lipid-membrane binding. In the crystal structure, the geometry of these five hydrophobic residues is that of a hairpin. One hypothesis is that these C-terminal residues form an anchor for the lipid membrane bilayer, such that it restricts the freedom of the entire vinculin protein and "drags" the tail domain closer to the acidic phospholipid heads protruding from the surface of the membrane. Subsequent intermolecular hydrogen-bonding between the lipid heads and the basic residues of the vinculin tail could trigger the unfurling of the helical bundle, resulting in a tighter association of helix 3 (H3) with the acidic lipid heads [20,21]. Recent NMR data indicate that the removal of more than four amino acids perturbs the vinculin tail structure and significantly reduces acidic phospholipid binding of this domain [22]. These researchers claim that the C-terminal hydrophobic hairpin is not required for the association with PIP_2-containing liposomes. It was further reported that a defective interaction between the vinculin tail and the phospholipids impairs cell spreading, motility, stiffness, and tractions [3,6,23]. From these reports it is not clear, if these interactions are associated with the membrane and, therefore, this *in vitro* study focused specifically on the proposed lipid binding regions of the vinculin tail, i.e. the H3- and C-terminus region.

The general aim of the research here was to investigate membrane phospholipid interactions with the vinculin tail and specifically how those same interactions are aided by the H3- and C-terminal region. The work was divided in a study of biochemical and biophysical approaches, using differential scanning calorimetry (DSC), CD-spectroscopy, fluorescence quenching, and gel electrophoresis.

Differential scanning calorimetry is the most direct experimental technique to resolve the energy of conformational transitions of biological molecules. It provides an immediate access to the thermodynamic mechanism that governs a conformational equilibrium of proteins and lipids by measuring the temperature dependence of the heat capacity, and thus the transition enthalpy (ΔH). Here, DSC was deployed to describe and discriminate between the energetics of the vinculin tail phospholipid association and insertion for different lipid environments. Using this method, we examined the two regions of the vinculin tail, H3 and the C-terminus, of possible interactions with phospholipids. Results from these measurements showed that H3 associates with the surface of DMPC/DMPS vesicles probably by hydrogen-bonding and that the C-terminus inserts into the lipid bilayer. The phosphorylated form of the C-terminus (pY1065), however, interacts to a lesser degree with the membrane compared to CTwt. Previously, Chandrasekar et al. [3] demonstrated that a change in residues (R1060Q; K1061Q = CTmut) significantly impairs the interaction of the vinculin tail with vesicles containing 48% (PC):45% (PS):7% (PIP_2) phospholipids compared to wildtype (CTwt). Our measurements, however, showed similar lipid insertion potential for CTwt and CTmut with vesicles containing 70% (DMPC):30% (DMPS) (Fig. 4). Thus, when we increased the DMPS content of lipid vesicles, the insertion potential of CTmut decreased in comparison to CTwt peptides which support the observations by Chandrasekar et al. [3] (data not shown). As previously mentioned by Diez et al. [5], the increased hydrophobic moment of the C-terminal arm may explain why the lipid binding of vinculin tail (R1060Q/K1061Q) was suppressed, i.e. that a conformational change (in the vinculin tail lead-

ing to a buried C-terminus) could result in the loss of a membrane interaction site and in reduced lipid binding. This may also explain the discrepancy of this *in vitro* study and the results obtained *in vivo* by Diez et al. [6].

Among the biophysical techniques that allow the investigation of peptides and proteins in bilayer environments, CD spectroscopy has proven to be a valuable tool during the investigation of structure, dynamics, and topology. The strength of this method is to give accurate answers for specific questions, i.e. allowing measurements of large numbers of conformational constraints for complete structure determination of membrane-bound peptides. The CD-spectroscopic measurements here support DSC observations. Since the C-terminal region of vinculin is believed to exist in an unstructured configuration and protonating environment, this environment is similar to that found in solution with acidic phospholipids. Therefore, direct hydrogen-bonding to phospholipid headgroups is assumed for the H3 region, whilst the CT region is believed to insert into the lipid bilayer. Using freeze/thaw/centrifugation, i.e. pull-down assays and SDS–PAGE analysis further support the notion of vinculin's tail regions: H3 association and CT insertion with/into lipids.

5. Conclusions

Many proteins exist in soluble form in the cytoplasm and fractions may associate transiently with the boundary of the lipid membrane. In an aggregate form, proteins are likely to interact with lipids in a two-step mechanism: affinity driven by long range effects (electrostatic attraction and desolvation due to the hydrophobic effect) followed by selective interactions due to steric complementarity and stabilizing hydrogen-bonding contacts. Protein–lipid interactions are often associated with conformational changes that occur when the lipid molecules find complementary binding surfaces.

We believe that this study has provided more insight of the molecular biophysical behavior into the role of phospholipids that contribute to the turnover (assembly and disassembly) of adhesions. It supports the idea that the C-terminal region may improve the binding between the vinculin tail domain and phospholipid membranes and that the C-terminal region acts as an anchor ensuring that the vinculin tail domain interacts with phospholipid membranes. In summary, the results should give a better understanding into vinculin–lipid membrane interactions that contribute to cellular mechanical behavior, 2D cell migration, and 3D cell invasion [24–27].

Acknowledgments

We thank Dr. W.H. Ziegler for supplying vinculin tail constructs: H3 and CT and Drs. B. Fabry, B. Hoffmann, R. Sterner, and A. Kukol for stimulating discussions. This work was supported by grants from Bayerisch-Französisches Hochschulzentrum, Deutscher Akademischer Austausch Dienst, Bavaria California Technology Center, and Deutsche Forschungsgemeinschaft (GO598/13-1). VFW has been recommended for the Ohm prize of the university.

References

[1] D.L. Scott, G. Diez, W.H. Goldmann, Protein–lipid interactions: correlation of a predictive algorithm for lipid-binding sites with threedimensional structural data, Theor. Biol. Med. Model 3 (2006) 17.
[2] R.P. Johnson, V. Niggli, P. Durrer, S.W. Craig, A conserved motif in the tail domain of vinculin mediates association with and insertion into acidic phospholipid bilayers, Biochemistry 37 (1998) 10211–10222.
[3] I. Chandrasekar, T.E. Stradal, M.R. Holt, F. Entschladen, B.M. Jockusch, W.H. Ziegler, Vinculin acts as a sensor in lipid regulation of adhesion-site turnover, J. Cell Sci. 118 (2005) 1461–1472.
[4] C. Bakolitsa, J.M. De Pereda, C.R. Bagshaw, D.R. Critchley, R.C. Liddington, Crystal structure of the vinculin tail suggests a pathway for activation, Cell 99 (1999) 603–613.
[5] G. Diez, F. List, J. Smith, W.H. Ziegler, W.H. Goldmann, Direct evidence of vinculin tail–lipid membrane interaction in beta-sheet conformation, Biochem. Biophys. Res. Commun. 373 (2008) 69–73.
[6] G. Diez, P. Kollmannsberger, C.T. Mierke, T.M. Koch, H. Vali, B. Fabry, W.H. Goldmann, Anchorage of vinculin to lipid membranes influences cell mechanical properties, Biophys. J. 97 (2009) 3105–3112.
[7] W.H. Goldmann, B. Bechinger, T.P. Lele, Cytoskeletal proteins at the lipid membrane, in: H.T. Tien, A. Ottova-Leitmannova (Eds.), Planar Lipid Bilayers (BLM's) and their Applications, Elsevier Inc., Amsterdam, 2008, pp. 227–255.
[8] A.I.P.M. De Kroon, M.V. Soekarjo, J. De Gier, B. De Kruijff, The role of charge and hydrophobicity in peptide–lipid interaction: a comparative study based on tryptophan fluorescence measurements combined with the use of aqueous and hydrophobic quenchers, Biochemistry 36 (1990) 8229–8240.
[9] M.R. Eftink, C.A. Ghiron, Exposure of tryptophanyl residues in proteins. Quantitative determination by fluorescence quenching studies, Biochemistry 15 (1976) 672–680.
[10] V. Schewkunow, K.P. Sharma, G. Diez, A.H. Klemm, P.C. Sharma, W.H. Goldmann, Thermodynamic evidence of non-muscle myosin II–lipid membrane interaction, Biochem. Biophys. Res. Commun. 366 (2008) 500–505.
[11] B.R. Lentz, K.W. Clubb, D.R. Alford, M. Hoechli, G. Meissner, Phase behavior of membranes reconstituted from dipentadecanoyl-phosphatidylcholine and the magnesium-dependent, calcium-stimulated adenosine triphosphatase of sarcoplasmic reticulum: evidence for a disrupted lipid domain surrounding protein, Biochemistry 24 (1985) 433–442.
[12] F.J. Alenghat, B. Fabry, K.Y. Tsai, W.H. Goldmann, D.E. Ingber, Analysis of cell mechanics in single vinculin-deficient cells using a magnetic tweezer, Biochem. Biophys. Res. Commun. 277 (2000) 93–99.
[13] W.H. Goldmann, D.E. Ingber, Intact vinculin protein is required for control of cell shape, cell mechanics, and *rac*-dependent lamellipodia formation, Biochem. Biophys. Res. Commun. 290 (2002) 749–755.
[14] E. Papagrigoriou, A.R. Gingras, I.L. Barsukov, N. Bate, I.J. Fillingham, I.B. Patel, E. Frank, W.H. Ziegler, G.C. Roberts, D.R. Critchley, J. Emsley, Activation of a vinculin-binding site in the talin rod involves rearrangement of a five-helix bundle, EMBO J. 23 (2004) 2942–2951.
[15] V. Vogel, M.P. Sheetz, Local force and geometry sensing regulate cell functions, Nat. Rev. Mol. Cell Biol. 7 (2006) 265–275.
[16] W.H. Goldmann, M. Schindl, T.J. Cardozo, R.M. Ezzell, Motility of vinculin-deficient F9 embryonic carcinoma cells analyzed by video, laser confocal, and reflection interference contrast microscopy, Exp. Cell Res. 221 (1995) 311–319.
[17] W.H. Goldmann, Mechanical aspects of cell shape regulation and signaling, Cell Biol. Int. 26 (2002) 313–317.
[18] W.H. Goldmann, The coupling of vinculin to the cytoskeleton is not essential for mechano-chemical signaling in F9 cells, Cell Biol. Int. 26 (2002) 279–286.
[19] M. Tempel, W.H. Goldmann, G. Isenberg, E. Sackmann, Interaction of the 47-kDa talin fragment and the 32-kDa vinculin fragment with acidic phospholipids: a computer analysis, Biophys. J. 69 (1995) 228–241.
[20] C. Bakolitsa, D.M. Cohen, L.A. Bankston, A.A. Bobkov, G.W. Cadwell, L. Jennings, D.R. Critchley, S.W. Craig, R.C. Liddington, Structural basis for vinculin activation at sites of cell adhesion, Nature 430 (2004) 583–586.
[21] W.H. Ziegler, R.C. Liddington, D.R. Critchley, The structure and regulation of vinculin, Trends Cell Biol. 16 (2006) 453–460.
[22] S.M. Palmer, M.P. Playford, S.W. Craig, M.D. Schaller, S.L. Campbell, Lipid binding to the tail domain of vinculin, J. Biol. Chem. 284 (2009) 7223–7231.
[23] R.M. Saunders, M.R. Holt, L. Jennings, D.H. Sutton, I.L. Barsukov, A. Bokov, R.C. Liddington, E.A. Adamson, G.A. Dunn, D.R. Critchley, Eur. J. Cell Biol. 85 (2006) 487–500.
[24] C.T. Mierke, P. Kollmannsberger, D. Paranhos-Zitterbart, J. Smith, B. Fabry, W.H. Goldmann, Mechano-coupling and regulation of contractility by the vinculin tail domain, Biophys. J. 94 (2008) 661–670.
[25] C. Möhl, N. Kirchgeßner, C. Schäfer, K. Küpper, S. Born, G. Diez, W.H. Goldmann, R. Merkel, B. Hoffmann, Becoming stable and strong: the interplay between vinculin exchange dynamics and adhesion strength during adhesion site maturation, Cell Motil. Cytoskeleton 66 (2009) 350–364.
[26] C.T. Mierke, P. Kollmannsberger, D. Paranhos-Zitterbart, G. Diez, T.M. Koch, S. Marg, W.H. Ziegler, W.H. Goldmann, B. Fabry, Vinculin facilitates cell invasion into 3D collagen matrices, J. Biol. Chem. 285 (2010) 13121–13130.
[27] W.H. Goldmann, Correlation between the interaction of the vinculin tail domain with lipid membranes, its phosphorylation, and cell mechanical behaviour, Cell Biol. Int. 34 (2010) 339–342.